Commun. Math. Phys. 67, 93–108 (1979)

Communications in Mathematical Physics

Preturbulence: A Regime Observed in a Fluid Flow Model of Lorenz*

James L. Kaplan[1] and James A. Yorke[2]

[1] Department of Mathematics, Boston University, Boston, Massachusetts 02215, USA
[2] Institute for Physical Science and Technology and Department of Mathematics, University of Maryland, College Park, Maryland 20742, USA

Abstract. *This paper studies a forced, dissipative system of three ordinary* differential equations. The behavior of this system, first studied by Lorenz, has been interpreted as providing a mathematical mechanism for understanding turbulence. It is demonstrated that prior to the onset of chaotic behavior there exists a preturbulent state where turbulent orbits exist but represent a set of measure zero of initial conditions. The methodology of the paper is to postulate the short term behavior of the system, as observed numerically, to establish rigorously the behavior of particular orbits for all future time. Chaotic behavior first occurs when a parameter exceeds some critical value which is the first value for which the system possesses a homoclinic orbit. The arguments are similar to Smale's "horseshoe".

Section 1. Introduction and Definitions

Many mathematical attempts have been made to interpret the phenomenon of turbulence in fluids. Typically, the behavior of the fluid is represented by the trajectories of a system of differential equations and the system is assumed to depend on a parameter r. The parameter r usually corresponds to the Rayleigh or Reynold's number. [For a more detailed discussion of alternate interpretations of turbulence refer to [1].]

One of the most intriguing models of this type was studied by Lorenz [2]. Lorenz considered the forced dissipative system

$$\begin{aligned} x' &= -\sigma x + \sigma y \\ y' &= -xz + rx - y, \\ z' &= xy - bz. \end{aligned} \tag{1.1}$$

These ordinary differential equations are an approximation to a system of partial differential equations describing finite amplitude convection in a fluid layer heated

* Research supported by NSF Grant MCS 76-24432

0010-3616/79/0067/0093/$03.20

from below. If the unknown functions in the partial differential equations are expanded in a Fourier series and all the resulting Fourier coefficients are set equal to zero except three, system (1.1) results. For $\sigma = 10$, $b = 8/3$, Lorenz found numerically that the system (1.1) behaves "chaotically" whenever the Rayleigh number r exceeds a critical value $r_2 \approx 24.74$; that is, all solutions are unstable and almost all of them are aperiodic, though there are an infinite number of periodic solutions of different periods. The chaotic behavior and sensitive dependence upon initial conditions of solutions of differential equations provides a mechanism for understanding turbulence. Guckenheimer [3] gives an example of a dynamical system whose behavior appears topologically identical to that of Lorenz's system; the Guckenheimer system is more easily analyzed. Williams [4] analyzes the pattern of winding and twisting exhibited by these flows. Higher dimensional analogues of this system have been studied in [5, 6].

Our goal in this paper is to demonstrate that prior to the onset of chaotic behavior there exists a "preturbulent state" where turbulent orbits exist but represent an exceptional set (measure zero) of initial conditions. Lorenz demonstrates chaotic dynamics; we ask where the chaos came from. Our methodology will be to utilize the general short term behavior of the system, determined numerically, and described in Sect. 2 to predict the behavior of particular orbits for all future time. In particular, we will show that chaotic behavior actually first occurs when r exceeds $r_0 \approx 13.926$. The value r_0 is the first value for which system (1.1) possesses a homoclinic orbit (that is a bounded nonperiodic orbit having the same positive and negative limit set). The justification of this claim in Sect. 3 will be based upon arguments similar to Smale's famous horseshoe [7], [8]. In some sense, subsequent to the appearance of a homoclinic orbit, system (1.1) contains a "broken horseshoe". For $r < r_0$ there are no periodic orbits, while for $r = r_0 + \varepsilon$ for small $\varepsilon > 0$, there are an infinite number of periodic orbits and an infinite number of bounded orbits which do not tend asymptotically to any rest point or periodic orbit.

Definitions 1.1. Let X be a space with a metric $d(\cdot,\cdot)$, let $E \subset X$, and let $\tau : E \to X$.

We say a set $C \subset E$ is *invariant* if $\tau(C) = C$.

We say C is (Liapunov) *stable* if for each $\varepsilon > 0$ there is a $\delta \in (0, \varepsilon]$ such that $d(x, C) \leqq \delta$ implies that for every positive integer n, $d(\tau^n(x), C) \leqq \varepsilon$, (that is "you stay close if you start sufficiently close to C").

We say C is *attracting* (or is an *attractor*) if for each x sufficiently close to C, $\tau^n(x)$ approaches C, that is $d(\tau^n(x), C) \to 0$ as $n \to \infty$. This careful separation of attraction from stability is standard in the study of topological dynamics and dynamical system. A well known example by Denjoy [9] of a differential equation on a torus T^2 emphasizes the need for this distinction. In his example there is a non-empty connected compact invariant set $C \neq T^2$ which is neither a point nor a periodic orbit, (nor in fact does it contain any rest points or periodic orbits) but it is an attractor (as defined above). Hence it is a "strange attractor". (A strange attractor was defined by Ruelle and Takens [10] to be in essence any compact connected attracting set which is neither a rest point nor a periodic orbit nor a surface of any dimension). However, it is not stable. The strange attractors of Ruelle and Takens [10] and Guckenheimer [3] and presumably Lorenz are stable; they should be called strange stable attractors. Since no definition of turbulence is universally accepted it is difficult to say

whether the existence of a strange attractor implies the existence of turbulence, but it is clear that Ruelle and Takens have identified a source of irregular and chaotic behavior.

We remark that the definition of the term "strange attractor" is based on the shape or geometry of an invariant set rather than the dynamics within that set. A number of examples have appeared which suggest the need for a detailed taxonomy based on the dynamics rather than the shape. In particular Lorenz argued that his attractor was chaotic by examining functions $\tau:[a,b]\to[a,b]$. In some of his examples, the entire interval exhibits chaotic dynamics. Certainly nothing about the "shape" of an interval suggests the nature of the dynamics.

We say that *the dynamics on C depends sensitively on initial conditions* if every trajectory in C is Liapunov unstable even when the dynamics are restricted to C; more precisely, for each $x\in C$, there is a $\varepsilon>0$ and a sequence $\{y_i\}\subset C$ with $y_i\to x$ such that for each y_i there is a positive $n(=n(i))$ for which $d(\tau^n(y_i),\tau^n(x))>\varepsilon$.

We say a compact invariant set C is *chaotic* if C is inherently unstable and there is a dense orbit in C; that is, the closure of the set $\{\tau^n(x):n=1,2,\ldots\}$ is C. If C has one dense orbit, then "most" points of C have dense orbits, provided "most" is interpreted in the topological sense of Baire Category (see [11], Theorem 9.20). The horseshoe example of Smale [7 or 12, Chap. 4] contains a chaotic set which is neither stable nor attracting. In this paper we will show that for certain "preturbulent" parameter values the Lorenz system has a chaotic set which is clearly neither stable nor attracting. Axiom A maps [8, 12] have attractors which display sensitive dependence on initial conditions.

We will say a flow has a chaotic set if some Poincaré "return" map has a chaotic set.

We carefully demonstrate the existence of the strange set only for values of r slightly above the critical value $r_0\approx 13.926$, but we would also like to describe what we seem to see over a wider range of r. The chaotic set we observe is a Cantor set of orbits, each orbit being a saddle. As r increases from r_0 to $r_1\approx 24.06$, the chaotic set grows in size, without any change in its topology. (This is in contrast to the infinitely many topological types of the chaotic stable attractor for $r>r_2$ [3]).

The Transition to Turbulence. We conducted the following experiments in collaboration with Yorke. For any initial point p (given r) we define $\sigma(p)$ to be the number of sign changes of $x(t)$, the coordinate of the solution that represents the angular velocity. This in essence counts the number of times the orbit switches from an oscillation around one critical point to an oscillation around the other. For various values of r we chose many points at random from the region near the non-attracting chaotic set. There was a striking dichotomy in the results when r was large $(22<r<r_1)$. While $\sigma(p)$ was found to be 0 or 1 for many of the randomly chosen points, many other points produced large values of $\sigma(p)$. In particular for points near any of the three critical points, $\sigma(p)$ is found to be 0 or 1. Excluding all those points for which $\sigma(p)$ was 0 or 1, the rest were roughly distributed according to a (discrete) exponential distribution, the mean of which appears to go ∞ as $r\to r_1$. At $r=23$, the mean of these $\sigma(p)$ values appears to be well over 100, but for r near 24 the computer time required for careful statistics becomes prohibitive, and it is this range that is most interesting.

For r slightly less than 24.06, we thus have "metastable chaos", that is, chaotic behavior which is observed to persist for a long but finite time. Physically, our preturbulent state would appear to be one in which there is an attracting state (two stable attracting points) and a complementary region in which orbits oscillate chaotically. The observed trajectories act as if there were a half life to their stay in the chaotic region; if a trajectory in the chaotic state is observed for time T, knowledge of T tells us nothing about how much longer it will remain in the chaotic region. As $r \to r_1$ there is little change in the apparent volume of the metastable chaotic region surrounding the strange set. For $r < r_1$, almost every point in the chaotic region will eventually be sucked toward one of the attracting critical points, but the mean number of preceding oscillations is large. As r passes beyond r_1, the mean time becomes infinite and "suddenly" the ill-defined chaotic region becomes the region of attraction of the strange attractor. Robbins [13] investigates the transition to turbulence and reports she observed (numerically) orbits in the Lorenz system and related systems which oscillate chaotically for quite a while before settling down. Her parameter values correspond to our situation with r slightly less than r_1. Based on analysis of piecewise linear mappings on the real line to approximate the dynamics of the Lorenz system, Robbins [13, Sect. 3] argues that for all $r \in (r_0, r_1)$ (using the notation in our analogous situation) there is an unstable periodic orbit, in agreement with our findings. The argues that for large r in (r_0, r_1) there are others which do not approximate a steady solution, and for larger r in (r_0, r_1), "the set of trajectories may become uncountable". Her method disagrees with our findings of chaos near r_0. This metastable chaos regime may have been observed physically; Creveling et al. [14] reports an experiment involving fluid flow through pipes in which over a hundred oscillations are observed before the oscillations become regular and damp out. The existence of metastable chaotic regimes in physical situations could appear turbulent, for metastable chaos can persist for long durations. It is particularly difficult to determine whether apparent chaos in experiments in fact represents actual turbulence or just metastable chaos.

Table 1. *A summary of the apparent range of behavior of* (1.1) *as determined by theory and computations.* We list the critical changes as r is varied. This list is calculated for $\sigma = 10$ and $b = 8/3$. Except for the number of rest points and their local stability properties, all assertions are based upon numerical data.

For $r < 1$, 0 is globally attracting.

$r = 1$ is a transition value.

For $r > 1$ there are 3 rest points.

For $r < 13.926$ all trajectories tend to one of the rest points.

$r = r_0 \approx 13.926$ is a transition value. There exist 2 homoclinic orbits, trajectories starting from and going to 0. (See Fig. 5).

For $r > 13.926$ there are infinitely many periodic orbits, and infinitely many "turbulent orbits" which do not converge to any point or periodic orbit.

$r = r_1 \approx 24.06$ is a transition value. The unstable orbits from 0 tend to asymptotically unstable periodic orbits. These two periodic orbits are saddles and the orbits are in the stable manifolds of these periodic orbits. See Fig. 2).

For $r > 24.06$ there is a chaotic stable attractor. Between 24.06 and 24.74 there exist a chaotic stable attractor and a pair of stable attracting rest points.

$r = r_2 \approx 24.74$ is a transition value.

For $r > 24.74$ there are no stable points.

For some much larger values of $r > 50$ Lorenz has found stable periodic orbits, and for such values no chaotic attractor is observed.

Lorenz mentioned the transition at $r=24.74$ since this is the critical point at which the two regions of attraction of the non-zero rest points shrinks out of existence. McCracken [15, pp. 141–148] shows that at $r=r_2$ the non-zero critical points are unstable. McLaughlin and Martin [5] espouse the view point that the nature of this bifurcation causes "an immediate transition to turbulence", which seems to underemphasize the fact that a chaotic was established earlier at r_1.

Section 2. A Description of the Lorenz System

In order to establish the asymptotic behavior of the solutions of (1.1), we must first provide a detailed description of its trajectories, based upon numerical studies. These studies were performed on the UNIVAC 1108. Following Lorenz, we investigate the case $\sigma=10$, $b=8/3$.

There are 3 steady state solutions for $r>1$.

$$0=(x, y, z)=(0, 0, 0)$$

and

$$c=(x, y, z)=(\sqrt{b(r-1)}, \sqrt{b(r-1)}, r-1)$$

$$c'=(x, y, z)=(-\sqrt{b(r-1)}, -\sqrt{b(r-1)}, r-1).$$

The origin has a two-dimensional stable manifold and a one-dimensional unstable manifold while for $r>r_0$, c and c' each have a one-dimensional stable manifold and a two-dimensional unstable manifold. A projection of the trajectories onto the $y-z$ plane for $r=28$ is shown in Fig. 1. Observe that a trajectory appears to spiral around one critical point in Fig. 1 until its distance from that critical point exceeds some critical distance. Thereafter, it spirals about the other critical point with increasing

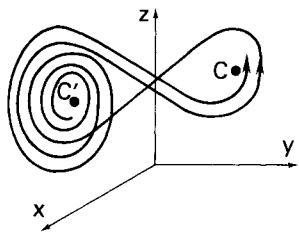

Fig. 1

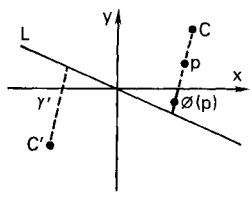

Fig. 2. The intersection of the stable manifold of 0 with the plane $z=r-1$. ϕ is not defined on this curve and ϕ changes discontinuously as this curve is crossed

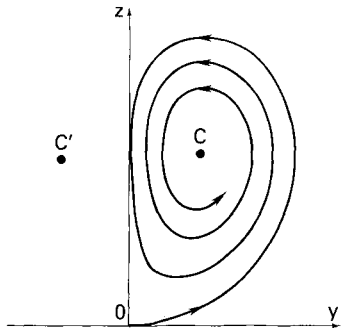

Fig. 3

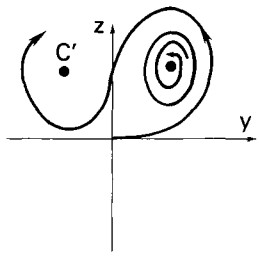

Fig. 4

oscillations until the critical distance is again exceeded. Trajectories at the critical distance lie on the stable manifold of 0.

In order to reduce the dimensionality of the problem we make use of a Poincaré map ϕ. Consider the plane $z=r-1$ containing c and c'. This plane is shown in Fig. 2.

The curve represents the intersection of the stable manifold of 0 with the plane $z=r-1$. ϕ is not defined on this curve and ϕ changes discontinuously as this curve is crossed. This discontinuity curve is almost straight.

Consider a point P in the plane and let $\phi(P)$ denote the first intersecting of the trajectory through P with the plane $z=r-1$ for which z is moving downward ($z'<0$). Successive images of a point P by ϕ tend to lie along the curves γ and γ'. For $r>r_2$, the curve γ represents the intersection of the plane with a medium-sized piece of the unstable manifold of the critical point. For $r<r_2$, there is no unstable manifold. Nevertheless, we can observe numerically the existence of a stable curve which is the analog of the curve in the case $r>r_2$, although we cannot prove that the curve exists. Moreover, since c and c' are unstable $\phi(P)$ lies further from c along γ than P. The curved line L is singular for the mapping ϕ. Orbits passing through L go to the critical point 0. For a detailed discussion of the trajectories of (1.1) for $r=28$, refer to the original paper by Lorenz [2]. A discussion of the Poincaré map ϕ when $r=28$ may be found in the recent paper by Ruelle [16].

As indicated previously we are concerned with the behavior of trajectories when r exceeds the critical value r_0.

Again, we consider a projection of the trajectories of system (1.1) onto the $y-z$ plane. When $r<r_0$ we observe the behavior shown in Fig. 3.

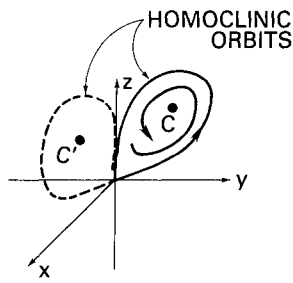

Fig. 5

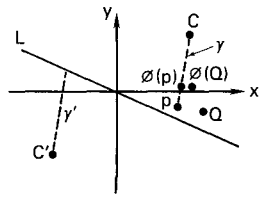

Fig. 6

Note that since system (1.1) is invariant under the transformation

$$(x, y, z) \to (-x, -y, z) \tag{2.1}$$

it is sufficient simply to draw the trajectories about c. The corresponding orbits about c' may be obtained by symmetry. The fixed points c and c' are asymptotically stable when $r < r_2$.

For $r > r_0$ the projection of trajectories of (1.1) onto the $y-z$ plane is substantially altered. The critical point c (and, of course, c') is still asymptotically stable (for $r < r_2$). For $r < r_1$ solutions outside an unstable trajectory from 0 can "cross-over" the z-axis in the $y-z$ plane and spiral into c'. See Fig. 4.

A comparison of Figs. 3 and 4, combined with the continuous dependence of solutions upon the parameter r, reveals that there must exist a transition value of r, which we have denoted by r_0, for which (1.1) possesses a homoclinic orbit. Intuitively, this is the value at which the transition takes place between the situation shown in Fig. 3, where a trajectory originating near the origin ultimately spirals about c, and that shown in Fig. 4, where a similar trajectory crossed over the z-axis. In the $y-z$ plane, we have Fig. 5.

Let us look at the Poincaré map ϕ associated with the parameter value r_0. The curve L again represents the intersection of the stable manifold with the plane $z = r_0 - 1 \approx 12.926\ldots$, and is a singular curve for the mapping. The image of a point P situated on γ will also be on γ, but closer to c. This is illustrated in Fig. 5, where we observe that c attracts all solutions originating "inside" the homoclinic orbit; if we examine a surface containing c and the spiral.

A point Q at the same distance from L as P, but not lying on γ, will be mapped to a point $\phi(Q)$ very near to $\phi(P)$. [We will discuss why this should be so shortly.]

We next consider the Poincaré map associated with the situation shown in Fig. 4 for r slightly greater than r_0. An initial point P_1 on γ near c is mapped closer to c along

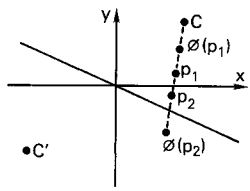

Fig. 7. Poincaré map on the plane $z=r-1$, $r>r_0$, $r<r_2$

γ, since c is still asymptotically stable. A point P_2 near L, however, is mapped across L. This is because a trajectory originating at P_2 near the stable manifold must pass very close to the origin. But, as we see in Fig. 4, any trajectory passing very close to the origin must cross over the stable manifold.

Suppose now that we parametrize the curve γ by arc length, taking the intersection of γ and L as our reference point. For any point P on γ we will denote by $\alpha(P)$ the length of γ between L and P, with $\alpha(P)$ being positive if P is on the same side of L as c. It is easily seen (refer to Fig. 7) that

$$\alpha(P_1)<\alpha(\phi(P_1))$$

while

$$\alpha(P_2)>\alpha(\phi(P_2))\,.$$

By the Intermediate Value Theorem there must exist some point P on γ between P_1 and P_2 for which

$$\alpha(P)=\alpha(\phi(P))\,.$$

But since α is one-to-one, this is equivalent to

$$P=\phi(P)\,.$$

Such a fixed point of the Poincaré map corresponds to the existence of a periodic solution of system (1.1).

We would like to examine an alternate approach to establishing the existence of a periodic solution of system (1.1) when $r>r_0$. This method has two primary advantages over the previous discussion:

(i) We will only need to consider the *local* behavior of the mapping ϕ in the neighborhood of L, rather than the behavior along the entire curve γ. These local properties are easily verified numerically simply by integrating the system (1.1) by computer.

(ii) Our new approach will be sufficiently general to allow us to establish in the next section the existence of an infinite number of periodic solutions of different periods, as well as an uncountable number of aperiodic orbits.

Consider an approximately rectangular region A as shown in Fig. 8. One long side of A, of length ε, lies along L and is centered at the intersection of L and γ. Denote its endpoints by P_1 and P_2, respectively. The other side of A is parallel to P_1P_2 and distance ε^2 away. The two shorter sides of A, P_1P_4 and P_2P_3, are normal to L at P_1 and P_2, respectively. Here ε is a small positive number.

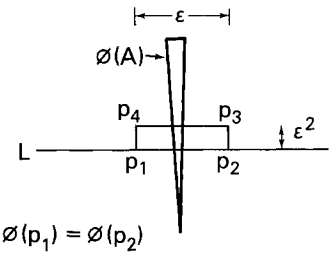

Fig. 8

What is the image of the region A under ϕ? We observe numerically that there exists some $\varepsilon_0 > 0$, such that for $\varepsilon \geqq \varepsilon_0$, the image of the point P_4, $\phi(P_4)$, lies much closer to c and nearer to γ. The point $\phi(P_3)$ is situated symmetrically across γ.

The mapping ϕ is not defined along L and so we cannot compute $\phi(P_1)$ and $\phi(P_2)$. However, we can determine $\lim_{\tilde{P}_1 \to P_1} \phi(\tilde{P}_1)$ and $\lim_{\tilde{P}_2 \to P_2} \phi(\tilde{P}_2)$ where the limits are taken over points $\tilde{P}_i$ which approach P_i, $i = 1, 2$, in A. Consider first a point $\tilde{P}_i$ in A near P_1. Such a point is mapped by the flow close to the origin. If it is sufficiently near to L initially we have already seen (see Fig. 4) that its trajectory will cross over the stable manifold, so that the point $\phi(\tilde{P}_1)$ will lie on the other side of L. Similar reasoning applies to the point $\phi(\tilde{P}_2)$. In fact, the closer the points $\tilde{P}_1$ and $\tilde{P}_2$ are to L initially, the closer together their trajectories will be near the origin. It follows that their images under ϕ can be made arbitrarily close, provided we choose $\tilde{P}_1$ and $\tilde{P}_2$ sufficiently near L. Of course, the points P_1 and P_2 are in no way distinguished (except for the fact that they lie on L). Thus, there exists a point Q (the point of intersection of an orbit originating near 0 on the unstable manifold with the plane $z = r - 1$) such that

$$Q = \lim_{\substack{P \to L \\ P \in A}} \phi(P) \tag{2.2}$$

We remark that it is because of (2.2) that we must have $\varepsilon \geqq \varepsilon_0 > 0$ (that is, ε cannot be too small). Otherwise, $\phi(P_3)$ and $\phi(P_4)$ would also lie near 0.

Notice in Fig. 8 that we have depicted $\phi(A)$ having substantially smaller area than A. Actually, the figure substantially exaggerates the area of $\phi(A)$. Lorenz observed the divergence is constant; hence the flow defined by system (1.1) contracts volumes in R^3 at the constant rate of

$$\frac{\partial \dot{x}}{\partial x} + \frac{\partial \dot{y}}{\partial y} + \frac{\partial \dot{z}}{\partial z} = -(\sigma + b + 1).$$

For the parameters we are considering this is -13.7, which is a very fast rate of contraction. Since it takes slightly more than 1 time unit for a trajectory originating on the plane $z = r - 1$ to intersect that plane again, it follows that the area of $\phi(A)$ will be approximately $e^{-13.7} \approx 10^{-6}$ times the area of A. This accounts for our difficulty in drawing our sketch to scale in Fig. 8.

The one-sided limit (2.2) enables us to extend the definition of ϕ to all of A. An examination of Fig. 8 now shows that the degree of the mapping ϕ on A is nonzero

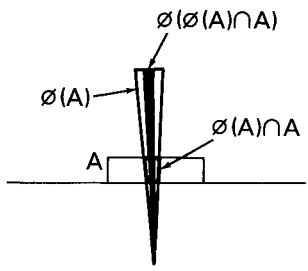

Fig. 9

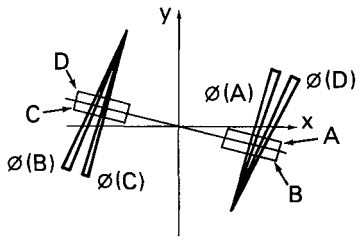

Fig. 10

and thus there must exist a fixed point of ϕ in A. This is in agreement with our previous reasoning.

Remark 2.1. Consider the "subrectangle" $\phi(A)\cap A$. Since two of its sides lie along P_1P_2 and P_3P_4, respectively, we must have that $\phi(\phi(A)\cap A)$ is stretched transversely across A, in a manner similar to $\phi(A)$.

Next we construct four rectangles, which we denote by A, B, C and D. We numerically computed their images under the Poincaré map ϕ, in a manner analogous to that described above. The results of our computations are shown in Fig. 10. We emphasize again that these results are obtained empirically.

In the next section we will show directly how the situation shown above implies the existence of an infinite number of periodic solutions of (1) with different periods, as well as an uncountable number of aperiodic orbits.

Remark 2.2. Smale's famous "horseshoe" example [7, 8] proved that if g is a diffeomorphism of the plane which possesses a transverse homoclinic orbit then it must contain a horseshoe. That is, there exists a rectangle R which is stretched linearly in the horizontal direction and contracted vertically then it is bent across R, as shown in Fig. 11. Here $g(p)=p'$ etc. The existence of the horseshoe, in turn, implies that g must have an infinite number of periodic points of different periods as well as an uncountable number of aperiodic points. Actually, in the analysis of the horseshoe it is not necessary to consider the action of g upon the entire rectangle R. It is sufficient to consider the behavior of g on the subrectangles A and B which are chosen so that $g(A)=\alpha$ and $g(B)=\beta$.

This observation has been utilized successfully by Guckenheimer, Oster and Ipaktchi [17] in which they study various higher dimensional difference schemes.

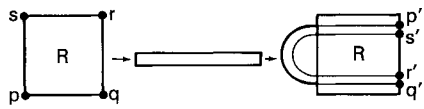

Fig. 11

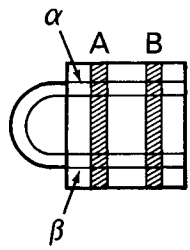

Fig. 12

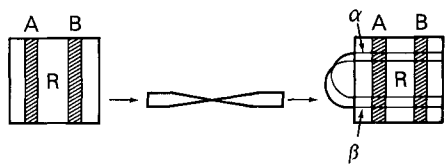

Fig. 13

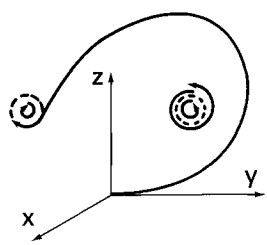

Fig. 14

They demonstrated numerically the existence of a "twisted" horseshoe. A rectangle R is again stretched linearly in the horizontal direction and contracted strongly vertically. Then, it is given a half twist before it is bent double across R. According to the remark we made above, the twist does not significantly alter the analysis of the mapping g on the subrectangles A and B. (cf. Figs. 12 and 13.) Once this identification is made, the authors are able to appeal to Smale's work to establish the existence of an infinite number of distinct periodic orbits, as well as an uncountable number of aperiodic ones. In the terminology of Ruelle and Takens, aperiodic orbits of this type are *turbulent* because their limit sets are neither points, nor periodic orbits, nor manifolds. Let us return to the situation generated by system (1.1), shown in Fig. 10. Let us make use of the symmetry relation (2.1) for system (1.1) to identify A with C, and B with D. Then a redrawn Fig. 10 would look as follows. This is precisely Smale's

horseshoe, and, in fact, we could now appeal to his work to establish our desired behavior. Actually, however, since A and C and B and D are separated, we have a "broken horseshoe". In the next section, we will present arguments applicable directly to the broken horseshoe to conclude the desired asymptotic behavior of the trajectories of system (1.1).

Section 3. Analysis of the "Broken Horseshoe"

In the previous section we displayed graphically (see Fig. 10) the action of the mapping ϕ on the four rectangular regions A, B, C and D. We may summarize these empirical results in the following fashion:

$$\begin{aligned} &A \xrightarrow{\phi} A+B, \\ &B \xrightarrow{\phi} C+D, \\ &C \xrightarrow{\phi} C+D, \\ &D \xrightarrow{\phi} A+B. \end{aligned} \tag{3.1}$$

Thus, for example, $A \xrightarrow{\phi} A+B$ indicates that $\phi(A) \cap A \neq \emptyset$ and $\phi(A) \cap B \neq \emptyset$ (see Fig. 9). We can now represent the action of ϕ on the set of symbols $\{A, B, C, D\}$ as a "transition matrix":

$$\psi = \begin{array}{c} \\ A \\ B \\ C \\ D \end{array} \begin{array}{c} \begin{array}{cccc} A & B & C & D \end{array} \\ \begin{bmatrix} 1 & 1 & 0 & 0 \\ 0 & 0 & 1 & 1 \\ 0 & 0 & 1 & 1 \\ 1 & 1 & 0 & 0 \end{bmatrix} \end{array} \tag{3.2}$$

where

$$\psi_{ij} = \begin{cases} 1 & \text{if some point in state } i \text{ is mapped into state } j. \\ 0 & \text{otherwise.} \end{cases}$$

The second iterate of ψ, ψ^2, is easily computed to be

$$\psi^2 = \begin{bmatrix} 1 & 1 & 1 & 1 \\ 1 & 1 & 1 & 1 \\ 1 & 1 & 1 & 1 \\ 1 & 1 & 1 & 1 \end{bmatrix}.$$

Here $\psi_{ij}^2 = 1$ for all $1 \leqq i, j \leqq 4$, which signifies that there is precisely one path of length 2, starting at any state i and ending at state j. For example, consider $\psi_{13}^2 = 1$. This tells us that there is precisely one way to proceed in "two steps" from A to C, namely

$$A \longrightarrow B \longrightarrow C.$$

Observe that there is no other path of the form $A \to X \to C$, according to (3.1).

In a similar manner

$$\psi^3 = \begin{bmatrix} 2 & 2 & 2 & 2 \\ 2 & 2 & 2 & 2 \\ 2 & 2 & 2 & 2 \\ 2 & 2 & 2 & 2 \end{bmatrix}.$$

Thus, for example, since $\psi^3_{14} = 2$ there are precisely two paths of length 3 starting at A and ending at D;

$$A \longrightarrow B \longrightarrow C \longrightarrow D,$$

and

$$A \longrightarrow A \longrightarrow B \longrightarrow D.$$

By induction we can verify that, in general

$$\psi^k = \begin{bmatrix} 2^{k-2} & 2^{k-2} & 2^{k-2} & 2^{k-2} \\ 2^{k-2} & 2^{k-2} & 2^{k-2} & 2^{k-2} \\ 2^{k-2} & 2^{k-2} & 2^{k-2} & 2^{k-2} \\ 2^{k-2} & 2^{k-2} & 2^{k-2} & 2^{k-2} \end{bmatrix}, \qquad k = 2, 3, \ldots \tag{3.3}$$

The procedure for relating the symbolic mapping (3.1) to the dynamics is quite similar to that used by Smale [7] except that his horseshoe involved two symbols instead of four. For an excellent exposition of the details, see Nitecki [12, Chap. 4 "The Horseshoe"]. We omit proofs for Lemmas 3.1 and 3.2.

Definition 3.1. Let $E = A \cup B \cup C \cup D$. We have referred to A, B, C, and D as symbols and we say for example a point $p \in E$ "has symbol A" if $p \in A$. Corresponding to the sequence of points $\{\phi^i(x)\} \subset E$, there is a sequence $S = \{X_i\}$ where each X_i is A or B or C or D and $i \in \{0, \pm 1, \ldots, \pm k\}$ or $i \in \{0, 1, \ldots\}$ or $i \in \{0, \pm 1, \pm 2, \ldots\}$. In the latter case we say $S = \{\ldots X_{-1}, X_0, X_1, \ldots\}$ is a *bisequence.* We say S is *realizable* if for each X_i and X_{i+1}, there are points in X_i which are mapped by ϕ into X_{i+1}, (that is, $\phi(X_i) \cap X_{i+1}$ is nonempty). We will say q is a *realization of* S if $\phi^i(q) \in X_i$ for each i.

Lemma 3.1. *Given any realizable sequence S, the set of realizations is nonempty and compact. For each realizable bisequence S, there is precisely one realization q. The bisequence is periodic with period k, (i.e., $X_i = X_{i+k}$ for all i) (if and) only if its realization is a periodic point with period k.*

In particular there are an infinite number of periodic orbits of (1.1) with distinct periods for r slightly greater than r_0 since there are infinitely many distinct realizable bisequences.

Let $E_0 = \{q \in E : \phi^i(q)$ is defined and is in E for all $i = 0, \pm 1, \ldots\}$. E_0 is the set of points which are realizations of bisequences.

Lemma 3.2. *Let $q \in E_0$ and $q_i \in E_0$ for $i = 1, 2, \ldots$. Then $q_i \to q$ as $i \to \infty$ if and only if for each $k = 0, \pm 1, \ldots$, $\phi^k(q_i)$ and $\phi^k(q)$ have the same symbol for all but finitely many i.*

Corollary 3.1. *There are an uncountable number of points $p \in E_0$ which are not periodic and are not asymptotic to any periodic orbit.*

Proof. Clearly there are an uncountable number of distinct realizable bisequences $\{X_i\}$ for which the sequence $\{X_0, X_1, \ldots\}$ is not eventually periodic, and the realizations of such sequences are not asymptotic to any periodic orbits. □

Remark 3.1. In the language of symbolic dynamics, our previous discussion has established the existence of a mixing subshift of finite type [12].

Remark 3.2. The number of periodic orbits of period n is given by

$$\text{trace } \psi^n = 4 \cdot 2^{n-2} = 2^n.$$

These, of necessity, include all periodic orbits whose period divides n. In order to find the number of orbits having least period n we must subtract the number of orbits of period k for which k divides n. For example trace $\psi^3 = 2^3 = 8$, so that there are 8 orbits of period 3. The only factor of 3 is 1, and there are 2^1 one-cycles, namely $A \to A$ and $C \to C$. Thus there are $8 - 2 = 6$ orbits with least period 3, and these are easily found to be

$$A \to B \to D \to A,$$
$$B \to D \to A \to B,$$
$$D \to A \to B \to D,$$
$$C \to D \to B \to C,$$
$$D \to B \to C \to D,$$
$$B \to C \to D \to B.$$

This scheme counts the first three of these cycles separately, when in fact they represent the same orbit of (1). The same is true of the last three cycles. In order to find the number of distinct cycles we must therefore divide by the length of the cycle. In this case this yields the fact there are $\frac{8-2}{3} = 2$ distinct periodic orbits. The same type of reasoning can be used to enumerate the periodic orbits of ϕ of any order n.

Corollary 3.2. *The set E_0 is chaotic.*

Proof. To construct a dense orbit in E_0 let $S = \{X_i\}$ be a realizable bisequence such that for each finite realizable sequence of symbols $\{Y_{-k}, \ldots, Y_k\}$ there exists a positive integer n such that $X_{n+i} = Y_i$ for all $i = -k, \ldots, k$. Let q be the realization of S. For each p in E_0 and each k there is an $n = n(p, k) > 0$ such that for $i = -k, \ldots, k$, $\phi^{n+i}(q)$ and $\phi^i(p)$ have the same symbol; i.e., both are in the same set A, B, C, or D. Let $q_k = \phi^{n(k,p)}(q)$. It follows from Prop. 3.1 that $q_k \to p$ as $k \to \infty$. Hence the orbit of q is dense in E_0.

To see that E_0 is inherently unstable, let p be in E_0. Write $E_1 = A \cap E_0$, $E_2 = B \cap E_0$, $E_3 = C \cap E_0$, and $E_4 = D \cap E_0$. Let $\varepsilon_{ij} = \inf d(x, y)$ for $x \in E_i$ and $y \in E_j$. Let ε be the minimum of ε_{ij} for $i \neq j$. Notice that $\varepsilon > 0$ since points near $A \cap B$ or $C \cap D$ are mapped out of $A \cup B \cup C \cup D$. If y is any point in E_0 let $\{X_i\}$ be the corresponding bisequence. For $k = 1, 2, \ldots$ let $S_k = \{Y_{ik}\}$ be a realizable bisequence such that $Y_{ik} = X_i$ for all $|i| < k$

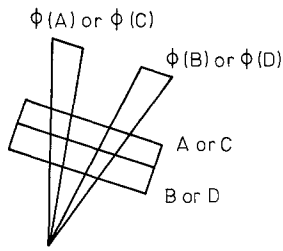

Fig. 15. At $r=r_1\approx 24.6$, the two trajectories emanating from (0, 0, 0) tend asymptotically to the (unstable) periodic orbits as shown. These periodic orbits are attracting in one dimension and repelling in one. For r smaller, the trajectory spirals into the critical point c'

and $Y_{kk}\neq X_k$. Let q_k^* be the realization of S_k. Then $q_k\to q$ and $q_k\in E_0$ but $d(\phi^k(q_k), \phi^k(q))>\varepsilon$, so E_0 is inherently unstable. □

We have now shown that for r immediately following the first appearance of a homoclinic orbit of (1.1) at $r=r_0$, there is an onset of chaotic behavior. For $r\in(r_0, r_1)$ the unstable orbits emanating from (0, 0, 0) reverse sides once (see Fig. 4 and then immediately spirals into a critical point (c' in the case of Fig. 4).

We seem to observe this entire structure persisting and growing until r reaches the next critical value, $r_1\approx 24.06$. Fig. 1 shows the critical picture.

Hence for $0<r\leqq r_1$, a homoclinic orbit occurs only for $r=r_0$.

References

1. Kaplan, J.L., Yorke, J.A.: The onset of chaos in a fluid flow model of Lorenz. Proc. NY Acad. Sci. (to appear)
2. Lorenz, E.N.: Deterministic nonperiodic flow. J. Atmos. Sci. **20**, 130–141 (1963)
3. Guckenheimer, J.: A strange attractor, in the Hopf bifurcation theorem and its applications. Marsden, J.E., McCracken, M. (ed.), pp. 368–381. Berlin, Heidelberg, New York: Springer 1976
4. Williams, R.F.: The structure of Lorenz attractors. Preprint (1977)
5. McLaughlin, J.B., Martin, P.C.: Transition to turbulence in a statically stressed fluid system. Phys. Rev. A **12**, 186–203 (1975)
6. Curry, J.H.: Transition to turbulence in finite-dimensional approximations to the Boussinesq equations. Ph. D. Thesis, University of California, Berkeley (1976)
7. Smale, S.: A structurally stable differentiable homeomorphism with an infinite number of periodic points. Proc. Int. Symp. Nonlinear Vibrations, Vol. II (1961); Izdat. Akad. Nauk. Ukrain SSR, Kiev (1963)
8. Smale, S.: Differentiable dynamical systems. Bull. Am. Math. Soc. **73**, 747–817 (1967)
9. Denjoy, A.: Sur les courbes défines par les équations différentielles à la surface du tore. J. Math. ser 9, **11**, 333–375 (1932)
10. Ruelle, D., Takens, F.: On the nature of turbulence. Commun. Math. Phys. **20**, 167–192 (1971); **23**, 343–344 (1971)
11. Gottschalk, W.H., Hedlund, G.A.: Topological dynamics, Vol. 36 (revised ed.). Providence, R.I.: Am. Math. Soc., Colloquium Pub. 1968
12. Nitecki, Z.: Differentiable dynamics. An introduction to the orbit structure of diffeomorphisms. Cambridge, Mass.: M.I.T. Press 1971
13. Robbins, K.A.: A new approach to subcritical instability and turbulent transitions in a simple dynamo. Math. Proc. Cambridge Phil. Soc.
14. Creveling, H.F., DePaz, J.F., Baladi, J.V., Schoenhals, R.J.: Stability characteristics of a single phase free convection loop. J. Fluid Mech. **67**, 65–84 (1975)

15. Marsden, J.E., McCracken, M.: The Hopf bifurcation and its applications. Berlin, Heidelberg, New York: Springer 1976
16. Ruelle, D.: The Lorenz attractor and the problem of turbulence. Proc. Conf. Quantum Dynamics Models and Mathematics, Bielefeld (1975)
17. Guckenheimer, J., Oster, G., Ipaktchi, A.: The dynamics of density dependent population models. J. Math. Biol. **4**, 101–147 (1977)

Communicated by J. Moser

Received April 21, 1977; in revised form September 1, 1978